Individual Vesicle Fusion Events Mediated by Lipid-Anchored DNA

Bettina van Lengerich,[△] Robert J. Rawle,[△] Poul Martin Bendix, and Steven G. Boxer*
Department of Chemistry, Stanford University, Stanford, California

ABSTRACT   Membrane fusion consists of a complex rearrangement of lipids and proteins that results in the merger of two lipid bilayers. We have developed a model system that employs synthetic DNA-lipid conjugates as a surrogate for the membrane proteins involved in the biological fusion reaction. We previously showed that complementary DNA-lipids, inserted into small uni-lamellar vesicles, can mediate membrane fusion in bulk. Here, we use a model membrane architecture developed in our lab to directly observe single-vesicle fusion events using fluorescence microscopy. In this system, a planar tethered membrane patch serves as the target membrane for incoming vesicles. This allows us to quantify the kinetics and characteristics of individual fusion events from the perspective of the lipids or the DNA-lipids involved in the process. We find that the fusion pathways are heterogeneous, with an arrested hemi-fusion state predominating, and we quantitate the outcome and rate of fusion events to construct a mechanistic model of DNA-mediated vesicle fusion. The waiting times between docking and fusion are distributed exponentially, suggesting that fusion occurs in a single step. Our analysis indicates that when two lipid bilayers are brought into close proximity, fusion occurs spontaneously, with little or no dependence on the number of DNA hybrids formed.

INTRODUCTION

Membrane fusion is central to many biological processes, including endo- and exocytosis and the transfer of membrane proteins between cellular compartments. The process of vesicle docking and fusion is mediated by formation of the SNARE protein complex, made up of recognition partners on the vesicle and target membranes, with many other accessory proteins assisting or regulating the process (1–3). Although extensively studied, essential questions about vesicle fusion, including the number of components involved and the precise physical mechanism, are not well understood and seemingly small differences in procedures and components among labs lead to different conclusions. Due to the complexity of the fusion reaction and the proteins involved, reductionist model systems can complement in vivo data to yield a better understanding of this biological process. Many such systems have been described that use the SNARE proteins (4–19) or synthetic surrogates for them (20–27), and these are providing valuable insight, as well as stimulating the development of increasingly realistic assays.

We have developed a model system (25–27) that employs synthetic DNA-lipid conjugates as surrogates for the SNARE machinery. This model system affords easy control over DNA sequence, binding geometry, and length—factors less easily probed in SNARE-mediated fusion—and it al-lows us to examine how fusion proceeds once the vesicle and target membrane are brought close together in the absence of accessory factors. The binding specificity of these DNA-lipid conjugates avoids having to deal with dead-end complexes due to promiscuous binding of incor-rect partners, and the conjugates spontaneously insert into lipid membranes without requiring detergent dialysis—two issues that can be troublesome in reconstituted SNARE systems (1,2,28). Hybridization of complementary DNA pairs on different membranes, when anchored in the correct orientation, enables fusion between small vesicles in bulk (25,26). Both lipid and content mixing are observed. Previ-ously, the mechanism of this multistep reaction could not be addressed as the kinetics of the docking and fusion reactions are convoluted in such ensemble measurements.

We recently developed a model membrane architecture—a DNA-tethered bilayer patch—that allows direct observa-tion of individual vesicle-to-planar bilayer fusion events to better investigate the mechanism of DNA-mediated vesicle fusion ((27), Fig. 1 A). In this system, we use DNA in two independent roles. The first is used to construct the target tethered patch with the DNA linked to the lipid anchor at its 5′ end on both surfaces—DNA hybridization in this configuration is referred to as the tethering orientation. A second, orthogonal DNA sequence is used to initiate vesicle docking and fusion, with the DNA anchored at its 3′ on one surface and its 5′ end on the other—hybridization between these strands is referred to as the zippering orientation and brings the membranes into close apposition to facilitate fusion. This is directly analogous to the proposed geometry of the docked SNARE complex at the presynaptic mem-brane (27,29), an improvement over many model systems that study fusion only between vesicles.

Herein, we use the information gathered from this system to construct a mechanistic model of the DNA-mediated fusion process and thereby provide insight into several important questions for the biological fusion reaction: Is fusion a linear pathway or is it heterogeneous? What is
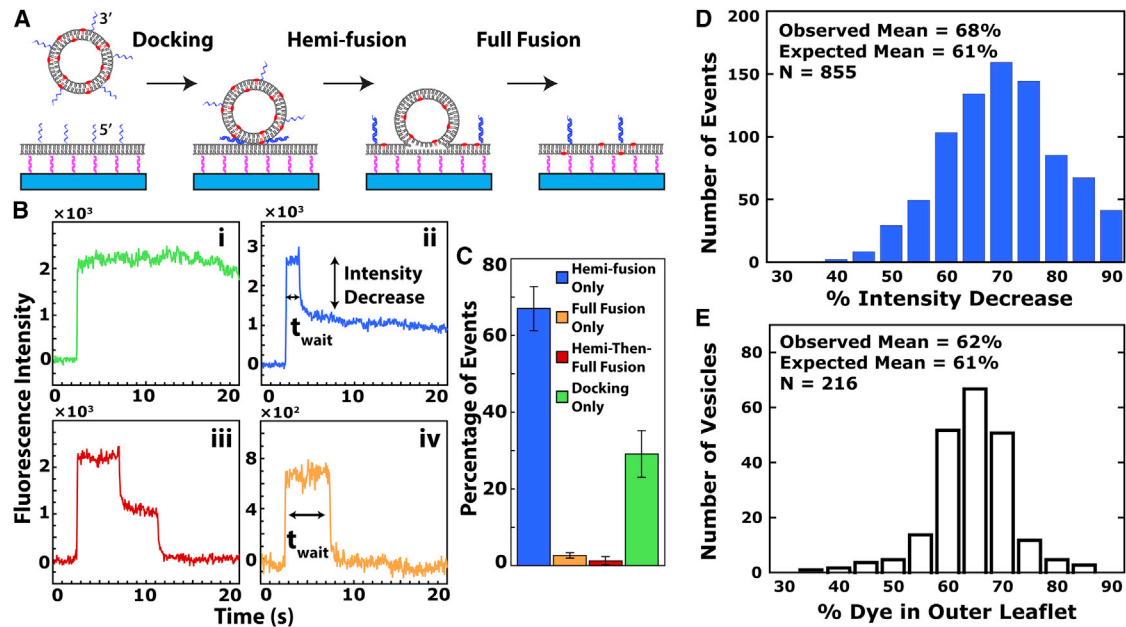
FIGURE 1   (A) Vesicle-to-tethered membrane patch assay. The target membrane patch, tens of μm in diameter, is tethered by 5′anchored 24mer DNA (*magenta strand*, 8 nm in height) to a modified glass coverslip, and also displays 5′anchored zippering DNA (*blue*) (27,30). DNA strands (*magenta* and *blue*) are on both leaflets of the tethered patch—not shown in the schematic to avoid confusion. A vesicle ~50 nm in diameter, with 2% Texas Red-labeled lipids (*red dots, both leaflets*) and displaying 3′coupled zippering DNA (*blue, outer leaflet only*) docks via DNA hybridization and then fuses to the tethered membrane patch, monitored by fluorescence microscopy. Nothing is drawn to scale. (B) Example traces of different fusion behaviors, showing the integrated fluorescence intensity in a ROI around each vesicle over time: (*i*) docking-only, (*ii*) hemi-fusion-only, (*iii*) hemi-then-full-fusion, (*iv*) full-fusion-only. (C) Proportions of fusion outcomes observed (65 DNA/vesicle, 3′PolyA). Error bars = STD of three experiments. To minimize sampling bias, only events that docked >60 s before the end of the 100 s video stream were included ($N > 400$ for all experiments). (D) The distribution of % intensity decrease upon hemi-fusion. (E) The distribution of % of dye-labeled-lipid in the outer leaflet of vesicles, as determined by dithionite quenching of NBD-PE fluorophores in the outer leaflet of DNA-tethered vesicles.

the role of hemi-fusion? How many binding partners are needed for fusion to proceed? Does DNA hybridization (or SNARE partnering) actively transduce zippering into membrane fusion? We observe that heterogeneous fusion behavior, with an arrested hemi-fusion state being the predominant outcome, emerges when the two membranes are brought into close apposition via DNA hybridization. The kinetics and fusion outcomes of the system are not substantially altered by the DNA sequence or number density on the vesicle and there is a gap of seconds between completion of DNA hybridization and a fusion transition. Furthermore, we observe that very few hybrids, possibly just one, are sufficient to allow this fusion behavior to proceed, and that the kinetics of the system are not greatly limited or enhanced by the formation of additional hybrids.

MATERIALS AND METHODS

Reagents

1,2-Dioleoyl-*sn*-glycero-3-phosphatidylcholine (DOPC), 1,2-dioleoylphosphatidyl-*sn*-glycero-3–ethanolamine (DOPE), and cholesterol (Ch) were purchased from Avanti Polar Lipids. Texas Red-DHPE and Oregon Green-DHPE were purchased from Invitrogen (Grand Island, NY). Ethynyl phosphonic acid and triethyl 2,2′,2′′′-(4,4′,4′′-nitrilotris(methylene)tris(1H-1,2,3-triazole-4,1-diyl))triacetate (TTMA) was generously provided by the

Chidsey lab at Stanford. DNA oligonucleotides were synthesized at the Protein and Nucleic Acid facility at Stanford.

Preparation of vesicles displaying DNA

DNA-lipids were prepared as in (25) by covalent attachment of a synthetic lipid-phosphoramidite as the final base to either the 3′ or 5′ end of an oligo on resin (sequences in Table S1), and subsequent purification on HPLC. Fluorescent dyes were conjugated to lipid-DNA postdeprotection using NHS chemistry (see the Supporting Material Section 1.1).

Vesicles were prepared by extrusion. A mixture of 2:1:1 DOPC/DOPE/Ch was dried from chloroform under a stream of nitrogen, then under vacuum for 3 h. For lipid mixing experiments, 2% Texas Red-DHPE (TR-DHPE) or 2% Oregon Green-DHPE (OG-DHPE) was also added. The lipid film was rehydrated to 0.4 mg/mL in 10 mM sodium phosphate, 240 mM sodium chloride buffer, pH 7.4 and extruded 29 times through a 30 nm polycarbonate membrane (Avanti Polar Lipids, Alabaster, AL). The resulting vesicle diameters were 48 ± 12 nm, measured by dynamic light scattering (Fig. S1). DNA-lipids (at tens of μM) were added to 5 μL of vesicles at 0.4 mg lipids/mL to yield the desired DNA density and are only displayed on the outer vesicle leaflet.

Giant unilamellar vesicles (GUVs) destined for tethered bilayers were made by gentle hydration (27). Their lipid composition was 2:1:1 DOPC/DOPE/Ch with 0.01% OG-DHPE added to locate the tethered membrane. They contained two different DNA-lipids (tethering strand: 0.5% Sequence 3, and zippering strand: sequence and concentration as specified). DNA-lipids are in both leaflets. For experiments using dye-labeled DNA, the OG-DHPE was left out. Instead, 0.01% dye-labeled DNA-lipid was included as the zippering strand.

Fusion experiments

A DNA-alkyne (Sequence 2-alkyne) was covalently attached to an alkyl azide-functionalized glass coverslip using click chemistry. GUVs with complementary tethering DNA (Sequence 1) and the specified zippering DNA were incubated with the substrate until the GUVs deformed and ruptured to form tethered bilayer patches, ~20–30 min (30). Membrane patches were thoroughly rinsed to remove any lipid debris and were characterized by uniformity of fluorescence and absence of lipid structures such as tubules. Once a suitable patch was located, vesicles (~10 μL at 1 μg lipids/mL) with the complementary zippering strand were added to the solution above the membrane patch. In the lipid mixing experiments (e.g., Fig. 1 A), docking was observed by appearance of a fluorescent, diffraction-limited vesicle on the patch. Hemi-fusion was observed by a sudden decrease of fluorescence within the vesicle region of interest (ROI) as some portion of its lipid dye was transferred to the target patch and rapidly diluted via diffusion. In full fusion, the fluorescence intensity completely disappeared (operationally defined as losing >90% of original intensity). Analysis was performed in a homemade MATLAB program (The MathWorks, Natick, MA). For all experiments, we only analyzed events >5 μm away from the edge of the tethered patch to avoid edge effects.

In the dye-DNA experiments (see Fig. 3 A), the tethered patches displayed 0.01% 5′PolyT-Alexa546 DNA-lipid and the vesicles displayed 3′PolyA DNA-lipid (and no lipid dye). Analysis and calculation of number of DNA hybrids formed is given in the Supporting Material Section 1.4.

NBD-dithionite quenching

Vesicles were prepared as previously mentioned, but containing 5% NBD-PE (headgroup labeled) instead of 2% TR-DHPE and displaying many 5′PolyT DNA lipids (~195 DNA/vesicle). These vesicles were tethered to an Egg PC glass supported lipid bilayer (SLB) displaying the complementary 5′PolyA DNA-lipids. This DNA-lipid pair will hybridize in the tethering orientation (cf. Fig. S7) and can form many hybrids, holding the vesicle immobilized and apart from the SLB membrane. After an initial fluorescence micrograph was taken of many tethered vesicles, 8 μL of 100 mM sodium dithionite was added to the ~40 μL solution above the vesicles. Following 2 min incubation, the chamber was rinsed with buffer and then a final micrograph was taken. A comparison of the initial and final fluorescence intensities of many vesicles yielded a distribution of percentage of NBD fluorophores in the outer leaflet (see Fig. 1 E).

Microscopy

All fusion experiments were performed on a Nikon Ti-U microscope with a 100× oil immersion objective (Nikon Instruments, Melville, NY; NA = 1.49). The excitation source was a Nikon Intensilight, which illuminated the sample uniformly using a liquid light guide. Images were recorded using an Andor iXon 897 (Andor Technology, Belfast, United Kingdom), and were processed with Metamorph software (Molecular Devices, Sunnyvale, CA). See the Supporting Material Section 1.3 for details on image acquisition and processing.

RESULTS

In a typical experiment, a dilute suspension of vesicles displaying DNA was manually pipetted into the solution above a tethered membrane patch displaying the complementary DNA sequence. Individual docking and fusion events were monitored via fluorescence microscopy by observing a lipid dye or a dye-labeled DNA-lipid. We previously observed that DNA-mediated fusion resulted in content transfer across the tethered bilayer and was distinguishable from vesicle rupture above the target bilayer (27), a common outcome observed by groups studying vesicle fusion to SLBs (15). These content transfer events were rare (~10%), therefore, in this report we focus on understanding the DNA-mediated fusion process from the perspective of the lipids and DNA-lipids. Using these fusion markers, we examined the fusion outcomes and kinetics, dependence on DNA sequence and number density, and behavior of DNA-lipids during fusion, each discussed separately below.

Fusion outcomes and kinetics

We first investigated the various fusion outcomes in lipid mixing experiments, in which we monitored the transfer of a lipid dye from vesicle to target patch (Fig. 1 A). The incoming vesicle displayed a moderately high density of DNA-lipids (65 DNA/vesicle, comparable to the reported number of ~70 synaptobrevin proteins on an average synaptic vesicle (31), as did the target bilayer (0.5 mol % or ~2500 DNA/μm^2 on the top-facing leaflet). The high density on the target ensures that the DNA-lipids will not become depleted during an experiment, in which hundreds of fusion events may occur on an individual patch. We analyzed the docking to fusion waiting times and behavior for hundreds of vesicles and observed four different outcomes following docking, classified as docking-only, hemi-fusion-only, hemi-then-full-fusion, and full-fusion-only—each discussed below. In control experiments, where we used noncomplementary sequences in the two membranes, or where the incoming vesicle contained no DNA-lipids, neither docking nor fusion was observed to occur (data not shown). Furthermore, if the tethering rather than zippering orientation of DNA was used to dock vesicles to the target bilayer, fusion did not occur (see the Supporting Material Section 7).

Docking-only

A substantial proportion of vesicles (~25–35%) were arrested following docking. These vesicles never transferred any of their lipid dye to the tethered patch during the experiment (Fig. 1 $B(i)$) and were classified as docking-only events. At least some docking-only events could be observed for hours without change, suggesting a rather permanently arrested docked state of the vesicle (see Fig. S2, b and d).

Hemi-fusion–only

The predominant behavior (~60–80%) of vesicles following docking was to transfer some, but not all, of their lipid dye to the tethered patch after some waiting time (t_{wait}, e.g., Fig. 1 $B(ii)$), and then to retain the remaining dye for the rest of the experiment. These events are classified as hemi-fusion-only. These hemi-fused vesicles appeared to be quite stable and could be observed for minutes and even hours without

undergoing any change in fluorescence intensity beyond photobleaching (Fig. S2, *a* and *c*).

To understand the docking to hemi-fusion transition, we performed a kinetic analysis of these events. Fig. 2 *A* shows the docking to hemi-fusion waiting times as a cumulative distribution function (CDF). This CDF could be fit to an exponential function using maximum likelihood estimation (mean waiting time $\tau_{wait} = 11.3$ s, 75 DNA/vesicle), suggesting that the transition from docking to hemi-fusion occurs in a single step.

To further characterize the hemi-fusion-only events, we quantified the percent decrease in fluorescence intensity upon hemi-fusion for hundreds of events (Fig. 1 *D*). Assuming that the lipid dye is distributed randomly between the inner and outer leaflets of the vesicle, we can estimate the expected mean percent intensity decrease upon hemi-fusion as the ratio of the outer to the total surface area of the vesicle. Using the average diameter of our vesicles

FIGURE 2 (*A*) Cumulative distribution function (CDF) of docking to hemi-fusion waiting times (*blue*) in vesicle-to-tethered membrane lipid mixing experiments (cf. Fig. 1A, 0.3 mol % 5′PolyT DNA-lipids in target membrane), with single exponential model (*black line*) fit by maximum likelihood estimation (see the Supporting Material Section 6). (*B*) CDFs across various average numbers of DNA/vesicle (1 to 65 DNA/vesicle, 3′PolyA). Complementary 5′PolyT DNA-lipids in the target membrane were kept constant at 0.5 mol %. See Table 1 for statistical data and Fig. S4 for actual DNA/vesicle distributions.

(48 ± 12 nm, measured by dynamic light scattering) and an estimated bilayer thickness of 5 nm, we calculated an expected mean percent intensity decrease of 61%.

Our observed mean (~68%) was near the expected mean, however the distribution was much wider than expected (~40–90%). Such wide-ranging values should not be possible for vesicles of reasonable size (vesicle diameter would need to be <20 nm to obtain a value of >80%, and values <50% should never be possible for a spherical vesicle). Although it is plausible that the wide distribution is due to nonrandom distribution of the lipid dye in the inner and outer leaflets, NBD-quenching of the lipid dye in the outer leaflet of tethered vesicles shows a narrow distribution of the percent dye in the outer leaflet (Fig. 1 *E*). Rather, it is possible that some apparent hemi-fusion events are in fact a transient merging of both leaflets, leading to a wider distribution of lipid dye transfer percentages than expected for pure hemi-fusion. Although this is a tentative interpretation, it is also consistent with our previous observation in content transfer experiments that some vesicles release only a portion of their contents during fusion events (27).

Hemi-then-full-fusion

Consistent with a canonical picture of vesicle fusion as proceeding from docking through a hemi-fused intermediate to full fusion (content transfer), we observed events that transferred a portion of their lipid dye to the tethered patch following docking, and then, after a further waiting period, transferred their remaining dye to the patch (Fig. 1 *B(iii)* and Movie S1). These events are classified as hemi-then-full-fusion events. Interestingly, these hemi-then-full-fusion accounted for <2% of events, even though this might be expected to be the canonical pathway. Because of their rarity, we performed no further analysis of these events.

Full-fusion–only

A small percentage (<5%) of vesicles transferred all their fluorescent dye to the target tethered membrane in one step, after a short waiting period following docking (Fig. 1 *B(iv)* and Movie S2). These are classified as full-fusion-only events because they appeared to transition directly to full fusion without passing through an observable hemi-fused intermediate.

Both the full-fusion-only and hemi-then-full-fusion events should result in content transfer across the tethered membrane. Together they account for ~5% of all events observed, consistent with our previous report (27) that DNA-mediated content transfer across a tethered patch was very rare—only ~10%. That report also showed that lipid-mixing and content transfer occurred simultaneously for our system (see Fig. 3 in (27)).

As with the hemi-fusion-only events, we performed a kinetic analysis of full-fusion-only events (N = 68), although their rarity means that this provides at best only
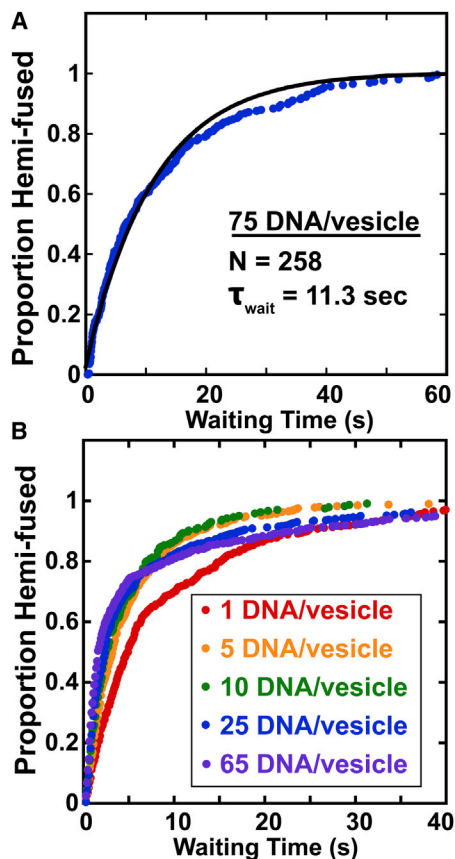
TABLE 1 Docking to hemi-fusion wait time statistics

DNA Sequence	Number density	Mean t_{wait}[a]	N[b]
Vesicle: 3′Poly A;	1 DNA/vesicle	9.3 ± 1.3 sec	369
	5 DNA/vesicle	5.3 ± 0.7 sec	410
	10 DNA/vesicle	4.8 ± 0.9 sec	248
Target: Poly T	25 DNA/vesicle	6.7 ± 1.1 sec	513
	65 DNA/vesicle	7.2 ± 1.2 sec	531

DNA Sequence	Number Density	Mean t_{wait}[a]	N
Vesicle: 3′ Seq 2;	5 DNA/vesicle	11.5 ± 2.0 sec	159
	10 DNA/vesicle	9.5 ± 2.1 sec	148
Target: Seq 1	25 DNA/vesicle	12.7 ± 2.6 sec	115
	65 DNA/vesicle	12.3 ± 2.1 sec	230

[a]Errors for the mean waiting time are 95% CI determined from bootstrap resampling of the docking to hemi-fusion wait times ($N_{bootstraps}$ = 10,000). The bootstrap distribution of mean waiting times was symmetrical on either side of the mean to within 0.2 s and the higher error estimate was chosen.
[b]N is the number of docking to hemi-fusion events in the data set.

an estimate of the full fusion kinetics. The CDF of the docking to full fusion wait times was also exponential (see Fig. S3), with an average waiting time of 15 s.

Dependence on number of DNA-lipids/vesicle

To examine the dependence of fusion on the number of available binding partners, we varied the number of DNA-lipids on the incoming vesicles from 65 DNA/vesicle to 1 DNA/vesicle (corresponding to 0.25 to 0.004 mol % DNA) while keeping the number density of DNA-lipids on the target tethered patch constant, and characterized the fusion behavior of vesicles at each number density.

Consistent with earlier work that quantified the rate of docking between mobile DNA-tethered vesicles with strands in the tethering orientation (32), we qualitatively observed that docking to the tethered patch (hybridizing in the zippering orientation) became rarer as the number of DNA/vesicle was reduced.

Surprisingly, decreasing the number of DNA/vesicle did not substantially alter the probability of achieving a certain fusion outcome, even at 1 DNA/vesicle. For all numbers of DNA/vesicle, hemi-fusion-only events predominated overwhelmingly, although interestingly we observed that docking-only events decreased to <10% for 1, 5, and 10 DNA/vesicle (data not shown) with a concomitant increase in hemi-fusion events. Even more surprisingly, and in contrast to conclusions inferred from bulk experiments (25,26), decreasing the number of DNA/vesicle did not dramatically alter the kinetics of the docking to hemi-fusion transition (Table 1 and Fig. 2 B). Down to 5 DNA/vesicle, the CDFs showed quite similar kinetic behavior with averages ~5–7 s. At 1 DNA/vesicle, the CDF was consistently slower, but the increase in average waiting time was not dramatic, increasing only to ~9 s.

In contrast to the fusion kinetics and outcome probabilities, the lateral mobility of the docked vesicles was significantly dependent on the DNA/vesicle number density (see Movie S3). At 65 DNA/vesicle, docked vesicles were mostly immobile; at 10 DNA/vesicle, some docked vesicles were slightly mobile; and at 1 DNA/vesicle, most docked vesicles were highly mobile on the surface of the tethered membrane. Presumably, mobility reflects the number of tethers formed between the vesicle and the tethered patch. However, the increased mobility of vesicles at lower numbers of DNA/vesicle did not hinder the transition to hemi-fusion. After diffusing for some time, mobile vesicles underwent hemi-fusion to the tethered patch and then remained fixed thereafter, presumably because the outer leaflet of the vesicle had merged with the tethered membrane, disallowing further diffusion.

Across several experiments, we observed that the slight pattern in the CDFs in Fig. 2 B for the number densities ranging from 65 to 5 DNA/vesicle appeared to be consistent and not entirely the result of experimental noise. A close inspection of these CDFs reveals that a slow population grows in at 25 and 65 DNA/vesicle, at which number densities the vesicles are immobile. This might indicate that having too many available tethers can actually inhibit the transition to hemi-fusion. A discussion of this, including kinetic models and fits to the data are outlined in the Supporting Material Section 5.

We note that the DNA/vesicle number densities in these experiments are the expected averages and are calculated using the average vesicle diameter (48 ± 12 nm). We confirmed that the actual average number density was near the expected average by using a dye-labeled DNA-lipid, but the width of a typical DNA/vesicle distribution is broad (Fig. S4). These distributions raise a potential issue for the limiting case of 1 DNA/vesicle, as the data may be biased toward the tail of the distribution via selection during docking. In that case, having 1 DNA/vesicle may not be enough to mediate fusion, or may only mediate it very slowly, but that would not be reflected in the data. As an approximate measure, the fusion of vesicles containing 0.25 DNA/vesicle on average, where by Poissonian statistics it would be rare for a vesicle to have >1 DNA, was measured (data not shown). For these vesicles, the docking rate is so low that it became impractical to collect statistical information, but we observed that docked vesicles could undergo hemi-fusion on timescales similar to the nominally 1 DNA/vesicle experiment. This issue is likely to complicate other reports of number dependence, and the best solution would be to work with populations of vesicles purified by the number of DNA (or SNARE)/vesicle (in progress).

Effect of DNA sequence

Previously, we observed that a PolyA/T repeating sequence mediated both faster vesicle-vesicle docking in individual vesicle docking measurements (32) and faster vesicle-vesicle fusion in bulk experiments (25) than a fully overlapping

sequence (Sequences 1 and 2 in Table S1). However, the docking study could not measure fusion, and the bulk experiments convolved docking and fusion, therefore it was not possible to discern the effect of DNA sequence on the fusion reaction. To determine how DNA sequence (and consequently the energetics of DNA hybridization) influences fusion behavior following docking, we performed lipid-mixing experiments as previously mentioned, but using Sequence 1 and 3′Sequence 2 ($T_m = 68.3°C$) as the zippering DNA strands (*blue strands* in Fig. 1 *A*) instead of the PolyA/T DNA sequences (Tm=55.3C). These TM values are calculated values for DNA oligomers (not DNA-lipids) in solution using the OligoAnalyzer tool on the www.idtdna.com website ([Na+] = 250 mM, [DNA] = 0.25 M (arbitrarily chosen)). The values are meant only to be a comparison demonstrating a difference in energetics of hybridization and cannot be directly extrapolated to DNA-lipid hybridization where the lipid anchors constrain the DNA to apposing membrane surfaces and the relevant concentration is the number density on each membrane. However, note that if the energy of DNA hybridization influences fusion behavior, DNA duplexes of the same length but with different T_m should exhibit different behavior.

Across four DNA/vesicle number densities (65, 25, 10, and 5 DNA/vesicle), only very moderate changes in kinetics or fusion outcomes were observed between the different DNA sequences. For the fully overlapping sequence, hemi-fusion-only was still the predominant outcome and the docking to hemi-fusion transition still followed exponential kinetics (Fig. S6), with an average wait time of ~10–12 s for all number densities (Table 1). This indicates that DNA sequence (and the energetics of DNA hybridization) does not strongly influence the fusion behavior of vesicles following docking; implying that the increased rate of fusion observed in bulk experiments (25) reflected a higher rate of docking, consistent with previous measurements of the sequence dependence of docking between individual tethered vesicles (32).

Also consistent with that implication, we observed that docking to the tethered patch was qualitatively much slower for the fully overlapping DNA sequence compared to the PolyA/T pair, presumably the result of increased geometrical constraints placed upon the fully overlapping sequences to initiate contact at the correct sequence location to successfully hybridize. This dramatically decreased docking rate made it impractical to collect data on vesicles containing 1 DNA/vesicle for the fully overlapping sequence, where docking became so rare that meaningful statistics could not be gathered.

Behavior of DNA-lipids during fusion

To gain insight into fusion from the perspective of the DNA-lipids, we investigated DNA hybrid formation subsequent to docking to determine how quickly and how many hybrids

form between the vesicle and target membrane. To accomplish this, DNA-lipids labeled at the membrane distal end with a fluorescent dye (typically Alexa546) were incorporated into the target tethered bilayer and the number of dye-labeled DNA-lipids that formed hybrids with a docked vesicle as illustrated in Fig. 3 *A* was quantified. In these experiments, the DNA-lipid density in the tethered patch is ~50 DNA-lipids per μm^2 on the top leaflet. To ensure that this lower density did not cause DNA-lipid diffusion to limit the observed rate of hybrid formation, we performed a simple calculation. The diffusion coefficient of lipids in the tethered membrane is ~5–6 μm^2/s (30). Assuming a similar diffusion coefficient for DNA-lipids in the target membrane, the encounter time of a DNA-lipid diffusing randomly on the patch with a docked vesicle is ~0.3 ms, and should not be rate-limiting. Likewise, a DNA-lipid diffusing randomly on a 50 nm vesicle will have a mean encounter time of <0.5 ms to reach any given target 5 nm in radius on the vesicle surface (33).

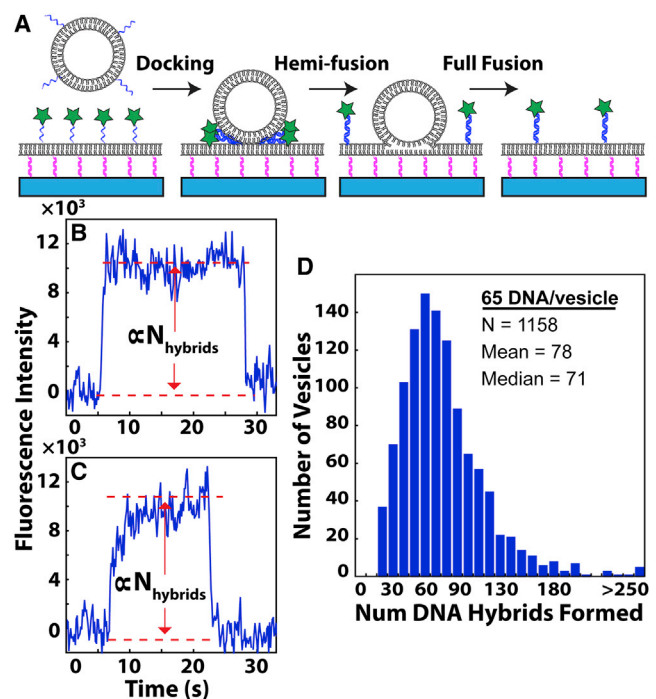FIGURE 3   (*A*) Schematic for DNA hybrid formation experiment. The tethered bilayer contains a low percent (0.01% ~100 DNA-lipids/μm^2) of Alexa546-5′PolyT (*green stars*), and the vesicles contain 3′PolyA. Docking is observed by the appearance of a spot as DNA hybrids form between tethered patch and vesicle, indicated by a (*B*) fast <1 s or (*C*) fast then slow (~10 s) rise in the intensity of the ROI against a dim background of laterally mobile-labeled DNA on the patch. Hemi/full fusion is detected by a sharp decrease in the intensity to baseline levels, as the labeled DNA-lipid hybrids diffuse into the much larger membrane patch area. DNA is displayed only on the outside of the vesicle, so hemi/full fusion is indistinguishable. (*D*) Distribution of the number of DNA hybrids formed between vesicle and tethered patch before undergoing hemi- or full fusion. Calculation of number of hybrids is given in the Supporting Material Section 1.4.

Before vesicle addition, the tethered bilayer has a dim, uniform background due to the rapidly diffusing dye-labeled DNA-lipids in the target patch. Upon vesicle docking (defined as the video frame in which a bright spot is first detected), dye-labeled DNA-lipids gather at the site of the docked vesicle as DNA-lipids on the vesicle hybridize to dye-labeled DNA on the target patch. This produces a local increase in the density of dye-labeled DNA at the site of the docked vesicle, resulting in a bright spot above the background (Fig. 3 B). The background-subtracted intensity of this spot is proportional to the number of DNA hybrids formed, which can be calculated using a calibration curve (see the Supporting Material Section 1.4). Due to the background created by the dye-DNA-lipids in the tethered patch (translated into DNA hybrid effective units, the noise is ~15 DNA hybrids for a vesicle-sized ROI), this experiment must be performed at high—65 and 42—DNA/vesicle densities. Upon hemi-fusion or full fusion (indistinguishable here), the spot rapidly disappears as the hybridized DNA duplexes diffuse into the membrane patch.

Two control experiments were performed. To verify the simultaneity of lipid transfer and DNA duplex release, we performed an experiment in which we monitored lipid mixing and DNA hybridization together, and observed that the release of the hybridized DNA duplexes into the membrane patch always coincided with a lipid transfer event (Fig. S9). To more directly measure DNA hybridization, we also performed a fluorescence resonance energy transfer experiment using a dye-labeled DNA on the vesicle and on the patch. As expected, the fluorescence resonance energy transfer ratio within a vesicle-sized ROI increased rapidly upon vesicle docking and diminished to background upon fusion (data not shown). However, we opted to use the one color hybridization experiment shown in Fig. 3 A for our analysis because of higher signal to noise.

When measuring how quickly hybrids form between vesicle and target membrane, we observed two behaviors (Figs. 3 B-C). For many vesicles, the intensity of the spot reached its maximum value in the initial frames upon docking, and then remained flat until fusion occurred. This indicates that most DNA hybrids formed rapidly upon docking (<1s), and that the number of hybrids remained constant during t_{wait} (Fig. 3 B). Other vesicles underwent a rapid rise in intensity during the first frames upon docking, but then the intensity slowly continued to rise for some longer time periods (often 10 s or more after docking, see Fig. 3 C). This suggests that many DNA hybrids are formed upon docking but then additional hybrids form more slowly over the next few seconds. The maximum number of hybrids formed did not seem to be correlated with the time it took to form them, suggesting that this slower accumulation of hybrids was not due to having more available tethers on the vesicle.

We next looked at the maximum number of hybrids formed by many docked vesicles and compared that to the number of DNA-lipids added, on average, to the vesicles (Fig. 3 D and Fig. S11). As expected, the distributions were wide (see the Supporting Material Section 4), but were surprisingly centered near the number added to the vesicles, suggesting that all DNA on the vesicles could hybridize with DNA on the tethered bilayer—as many as 60–70 duplexes on average in Fig. 3 D, with even higher numbers at the tail of the distribution. The minimum contact area between the vesicle and tethered bilayer that would be required to accommodate this many DNA hybrids was estimated by assuming that the duplexes hybridize completely and that they are equally spaced around the perimeter of the contact area. Then, if the width per duplex is 2 nm, a circular contact area of diameter >140 nm$/\pi = 44$ nm would minimally be required to accommodate 70 hybrids. Because the average diameter of our vesicles is ~50 nm, this suggests that the vesicles are greatly deformed and/or that incomplete hybridization (i.e., hybridization only at the membrane distal end) allows a staggered configuration of duplexes that would not require so large a contact area. Atomic force microscopy studies of vesicles adsorbed onto a glass surface have indicated that vesicles can deform quite dramatically upon adhesion, flattening to a width/height ratio of approximately five (34). Furthermore, recent cryo-electron microscopy images of tightly docked vesicles via SNARE complex formation suggest that such deformation may be possible for docked vesicles (Fig. 2 D and Fig. 3 C in (35)). It is also possible that the target membrane deforms locally to increase the contact area with the incoming vesicle, however similar results were obtained with SLBs as the target, a membrane that should be less deformable (data not shown).

DISCUSSION

In this study, we examined vesicle-to-tethered bilayer fusion events mediated by DNA-lipids (Fig. 1 A) as a model system for SNARE-mediated vesicle fusion. In our system, the incoming vesicles dock and fuse to a target membrane (tens of microns in diameter) that is held 8 nm from the surface by 24mer DNA tethers to minimize bilayer-surface interactions. This geometry mimics the curvatures of bilayers in the synapse, where synaptic vesicles (~40 nm in diameter, (31)) fuse to the locally planar plasma membrane. Using DNA-cholesterol conjugates, others have studied lipid-mixing events between vesicles and planar SLBs (36); using our DNA-lipid conjugates, we also observe lipid-mixing, but not content transfer between vesicles and SLBs (data not shown). Because content transfer is not observed (presumably due to bilayer-surface interactions, see also (15)), we prefer tethered bilayers to SLBs as planar target membranes.

Fig. 4 contains a graphical summary model of DNA-mediated vesicle fusion to a tethered bilayer based on the results described herein. Each state is discussed in detail below.
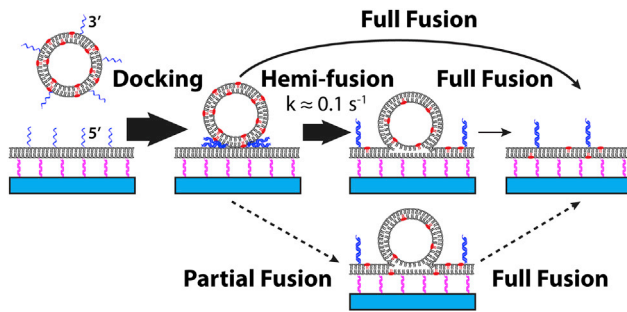
FIGURE 4 Graphical summary model of DNA-mediated fusion to a tethered patch. The locations of dye-labeled lipid molecules and DNA-lipids at each step reflect the understanding derived from the current study. The thickness of the arrows at each step represents the proportion of vesicles observed to undergo the various transitions. The dotted arrows to and from partial fusion represent our incomplete understanding of this transition—we have observed evidence of these transitions, but have not characterized them as a percentage of total events.

DNA hybrid formation and vesicle mobility upon docking

By assaying DNA hybrid formation during vesicle docking and fusion (Fig. 3), we observed that all available DNA-lipids on the vesicle (at least ~70/vesicle on average) can form hybrids with the target tethered patch. The number of DNA/vesicle (and consequently the number of hybrids formed upon docking) appears to govern the lateral mobility of the vesicle once docked to the tethered patch by DNA hybridization (Movie S3). As the number of DNA/vesicle decreases, vesicle mobility on the surface increases.

Vesicles arrested after docking

A significant proportion of vesicles with 65 DNA/vesicle (~25–35%, see Fig. 1 C) were arrested after docking. Vesicles arrested after docking have been observed in a variety of SNARE-based fusion model systems, with proportions varying widely from 0% to 90% (6,9,13,16–18). What causes these vesicles to become arrested remains unknown. One possibility is that fusion components (DNA-lipid, synaptobrevin, etc.) may become trapped between vesicle and target membranes, disallowing fusion by keeping the membranes apart. If this were the case, one would expect in our system that lower DNA/vesicle densities should produce fewer vesicles arrested after docking. At these lower densities, the vesicles are highly mobile and any trapped DNA-lipid could presumably easily escape or, in the case of a single hybrid, there would be no obvious mechanism to trap anything. Consistent with that expectation, we observed fewer docking-only vesicles (<10%) at low numbers of DNA/vesicle (data not shown). Lipid composition and vesicle curvature may also have a role in arresting vesicles after docking—these are discussed further in sections below.

Multiple fusion outcomes following docking

Several fusion outcomes were observed and are proportionately represented by the thickness of the arrows in Fig. 4. Most vesicles (*thick black arrow*) underwent hemi-fusion, where they were able to remain stable for minutes to hours (Fig. S2). <2% of hemi-fused vesicles (*thinnest black arrow*) later transitioned to full fusion and <5% (*medium black arrow*) of vesicles transitioned directly from docking to full fusion without passing through a measurable hemi-fusion intermediate. Based on the range of values observed for the percent intensity decrease upon lipid-mixing (Fig. 1 D), we inferred that there are also some partial fusion events in which both leaflets exchange momentarily with the target membrane—consistent with reports of transient fusion pore opening in SNARE-based systems (9,37,38) as well as partial content transfer events we observed previously (27). The exact proportion of such events, presumed to be small, is unknown (*dotted lines*). Surprisingly, the division among the various fusion pathways was not dramatically influenced by the DNA/vesicle number density or by the DNA sequence. Once the two membranes are brought close enough together, the various fusion behaviors emerge spontaneously, with hemi-fusion predominating in all cases. A very rough estimate of that distance, based on the width of a DNA duplex and linkage to the lipid anchor, is ~2–3 nm, although this distance could be even smaller should the duplex be pulled out of the way.

Other researchers have suggested that vesicle curvature may play an important role in determining fusion intermediates, kinetics, and outcomes (e.g. (39)). However, we did not observe a correlation between the initial intensities of the vesicles and the division among the fusion pathways or kinetics (data not shown), suggesting that the role of vesicle size and consequently curvature is not the major deciding factor in our data set, which only examined vesicles from a limited size distribution (Fig. S1). This is consistent with our observation that DNA-mediated fusion between mobile vesicles tethered to an SLB occurred on a similar timescale to fusion in our vesicle-to-tethered patch system (40).

Hemi-fusion kinetics and mechanistic implications

As the predominant outcome in our system, the hemi-fused state is of particular interest. Based on experiments monitoring lipid mixing (Fig. 1 D) and those monitoring dye-labeled DNA-lipids (Fig. 3 and Section 9 in the Supporting Material), we infer that this intermediate has fully exchanged its outer leaflet, including any DNA-lipids or hybrids, with the target membrane, as drawn in Fig. 4.

We observed that the CDFs for hemi-fusion wait times were exponential (Fig. 2), with k on the order of 0.1 s^{-1}. The CDF can reveal information on the number of steps

before fusion. If there are one or more steps before fusion (and if they occur on dissimilar timescales), the waiting times will follow a gamma distribution and the CDF will have an initial lag before rising. This has been observed in both SNARE-mediated and virus-mediated fusion of vesicles to planar bilayers, where the rate-limiting steps were attributed to the formation of more fusion pairs during the waiting time (6,41). A gamma distribution did not fit our CDFs at all, indicating that hybridization of DNA-lipids may be occurring much faster than protein binding in SNARE- or virus-based systems. In our system, the waiting time CDFs were always exponential, implying a stochastic process from docking to fusion.

Consistent with the implication that forming a certain number of DNA hybrids is not a rate-limiting step, the hemi-fusion rate was very similar across a wide range of DNA/vesicle and for different DNA sequences (Table 1). Vesicles with >1 DNA/vesicle underwent slightly faster hemi-fusion, with a possible minimum near 10 DNA/vesicle, but the difference was not dramatic, especially considering that docked vesicles with low DNA/vesicle densities were quite mobile—suggesting they were not held as closely to the target membrane as those with higher DNA/vesicle densities. Furthermore, the observation that many DNA hybrids could form shortly after vesicle docking and then remain constant in number until fusion occurred (Fig. 3 B) also suggests that DNA hybrid formation is not directly coupled to the fusion event. The lack of strong dependence of the rate of hemi-fusion on the sequence or number of DNA hybrids, in combination with the seconds timescale between docking due to hybridization and (hemi)fusion, suggests that the energy of DNA hybridization is not actively transduced into membrane fusion (hemi- or full) as any energy gained in the binding event is dissipated prior to the fusion event.

What, then, is the nature of the waiting time between docking and fusion? To explain slow SNARE-mediated vesicle-to-SLB fusion events on the order of seconds, others have suggested that local lipid tail fluctuations could initiate fusion between apposing membranes (12). In that case, the waiting time between docking and hemi/full fusion would be the time until a local lipid fluctuation occurred to initiate fusion. This mechanism, where lipid tails infrequently sample the polar interface leading to nucleation of a fusion pore, has been demonstrated in simulations, although only for highly constrained, curved vesicles on timescales much shorter than our experiments (42,43). This stochastic process should produce an exponential distribution of waiting times, consistent with our observations, but is difficult to verify experimentally.

Vesicles arrested after hemi-fusion

Vesicles arrested at hemi-fusion have been observed in other model systems, although typically at lower percentages than observed here (9,13). One explanation for why hemi-fusion

is the predominant endpoint of our system is that the lipid anchor of our DNA-lipids spans only one leaflet of the vesicle bilayer. The importance of the SNARE transmembrane domains for promoting full fusion has been suggested by a number of reports (10,14,44–47), although one study showed fusion could be achieved with the addition of several accessory proteins even if the SNARE transmembrane domain was replaced with an anchor spanning only one leaflet (44). Because our DNA-lipids only span half the bilayer, all hybridized pairs can diffuse into the target bilayer upon hemi-fusion, leaving the hemi-fused vesicle without any DNA-lipids as depicted in Fig. 4. This could explain why the hemi-fused state is the predominant endpoint in our system.

Lipid composition may also have a role to play in arresting the vesicles at hemi-fusion (or at docking). The particular lipid composition used here (2:1:1 DOPC/DOPE/Chol) was chosen based on other model membrane fusion systems (21) and because we observed the greatest extent of DNA-mediated lipid and content mixing in bulk experiments, while ensuring no leakage of vesicle contents or nonspecific fusion (25). However, this composition may stabilize the hemi-fused intermediate so that transition to full fusion becomes difficult. Indeed, other researchers have demonstrated that lipids with negative curvature (such as PE) can stabilize the hemi-fused intermediate (9,13,48), and removal of negatively curved lipids can in some cases lead to an increased propensity for full fusion events (13). PE is, however, a significant component of the synaptic vesicle lipid composition (31) suggesting that the biological fusion machinery must be able to overcome or avoid any hemi-fusion intermediates stabilized by lipid composition.

Implications for biological fusion

The conclusions emerging from our study of DNA-mediated fusion have several implications for the biological fusion reaction and lend support to several mechanistic proposals.

One, our data suggest there are multiple fusion pathways that can be accessed merely by bringing the vesicle and target membrane into close apposition upon DNA binding in the zippering orientation, and the kinetics of these processes imply a stochastic mechanism of fusion. This implies that the role of the biological fusion machinery is not just to encourage progression along a single trajectory toward content release, but rather to select from among several possible fusion pathways so that fusion will occur both properly and at the correct time, as recently proposed (5). In combination with our content mixing data (27) this also supports the idea that in biological fusion an inhibitory mechanism may exist in which docked vesicles are prevented from fusing until the correct moment (3). This inhibitory state could be achieved by holding the membranes and SNAREs a sufficient distance apart so they do not zipper until the correct moment, or by physically blocking the membranes from coming

into close proximity following SNARE zippering or partial zippering.

Two, our data support the emerging proposals that very few fusion-mediating complexes (DNA, SNAREs, etc.), possibly even just one, may be required to achieve the membrane proximity that allows fusion to occur (6,8,14), although in the biological system it is likely that other fusion components are necessary to encourage the correct fusion pathway at the right time. In our data, we observed that fusion behavior and kinetics were relatively unchanged down to one DNA/vesicle on average, suggesting that additional complexes do not play a significant role in driving fusion.

Three, our results suggest that the hemi-fused intermediate is actually quite stable and can be a predominant endpoint. The hemi-fused intermediate has been observed in pure lipidic systems (49), and recent data suggests that hemi-fusion may produce a kinetically trapped fusion state for synaptic vesicle fusion as well (5,35), indicating that a stable hemi-fused structure can occur across a variety of model systems.

Four, in contrast to mechanistic hypotheses that propose the zippering of the SNAREs is directly transduced into membrane fusion (e.g. (45)), our data show a lag time between DNA zippering and membrane fusion and suggests a stochastic mechanism. This may be a limitation of not having a transmembrane anchor for our DNA-lipids or it could suggest an alternate fusion mechanism.

Finally, an exponential distribution of wait times with an average of several seconds might be acceptable for some biological fusion pathways, but it is clearly too slow for the exquisite timing needed for synaptic vesicle fusion (1). Indeed, slower-than-expected fusion has been a problem in nearly all in vitro membrane fusion systems to date and a variety of accessory proteins have been suggested to be the principal timing mechanisms (50). Ultimately, this highlights the importance of further experimentation to understand the molecular mechanism of vesicle fusion.

SUPPORTING MATERIAL

REFERENCES

1. Brunger, A. T. 2005. Structure and function of SNARE and SNARE-interacting proteins. *Q. Rev. Biophys.* 38:1–47.

2. Rizo, J., and T. C. Südhof. 2012. The membrane fusion enigma: SNAREs, Sec1/Munc18 proteins, and their accomplices—guilty as charged? *Annu. Rev. Cell Dev. Biol.* 28:279–308.

3. Jahn, R., and D. Fasshauer. 2012. Molecular machines governing exocytosis of synaptic vesicles. *Nature.* 490:201–207.

4. Weber, T., B. V. Zemelman, …, J. E. Rothman. 1998. SNAREpins: minimal machinery for membrane fusion. *Cell.* 92:759–772.

5. Diao, J., P. Grob, …, A. T. Brunger. 2012. Synaptic proteins promote calcium-triggered fusion from point contract to full fusion. *eLife.* 1:e00109.

6. Domanska, M. K., V. Kiessling, …, L. K. Tamm. 2009. Single vesicle millisecond fusion kinetics reveals number of SNARE complexes optimal for fast SNARE-mediated membrane fusion. *J. Biol. Chem.* 284:32158–32166.

7. Karatekin, E., J. Di Giovanni, …, J. E. Rothman. 2010. A fast, single-vesicle fusion assay mimics physiological SNARE requirements. *Proc. Natl. Acad. Sci. USA.* 107:3517–3521.

8. van den Bogaart, G., M. G. Holt, …, R. Jahn. 2010. One SNARE complex is sufficient for membrane fusion. *Nat. Struct. Mol. Biol.* 17:358–364.

9. Yoon, T. Y., B. Okumus, …, T. Ha. 2006. Multiple intermediates in SNARE-induced membrane fusion. *Proc. Natl. Acad. Sci. USA.* 103:19731–19736.

10. McNew, J. A., T. Weber, …, J. E. Rothman. 2000. Close is not enough: SNARE-dependent membrane fusion requires an active mechanism that transduces force to membrane anchors. *J. Cell Biol.* 150:105–117.

11. Xu, H., M. Zick, …, Y. Jun. 2011. A lipid-anchored SNARE supports membrane fusion. *Proc. Natl. Acad. Sci. USA.* 108:17325–17330.

12. Domanska, M. K., V. Kiessling, and L. K. Tamm. 2010. Docking and fast fusion of synaptobrevin vesicles depends on the lipid compositions of the vesicle and the acceptor SNARE complex-containing target membrane. *Biophys. J.* 99:2936–2946.

13. Liu, T., T. Wang, …, J. C. Weisshaar. 2008. Productive hemifusion intermediates in fast vesicle fusion driven by neuronal SNAREs. *Biophys. J.* 94:1303–1314.

14. Shi, L., Q. T. Shen, …, F. Pincet. 2012. SNARE proteins: one to fuse and three to keep the nascent fusion pore open. *Science.* 335:1355–1359.

15. Wang, T., E. A. Smith, …, J. C. Weisshaar. 2009. Lipid mixing and content release in single-vesicle, SNARE-driven fusion assay with 1–5 ms resolution. *Biophys. J.* 96:4122–4131.

16. Fix, M., T. J. Melia, …, S. M. Simon. 2004. Imaging single membrane fusion events mediated by SNARE proteins. *Proc. Natl. Acad. Sci. USA.* 101:7311–7316.

17. Bowen, M. E., K. Weninger, …, S. Chu. 2004. Single molecule observation of liposome-bilayer fusion thermally induced by soluble *N*-ethyl maleimide sensitive-factor attachment protein receptors (SNAREs). *Biophys. J.* 87:3569–3584.

18. Liu, T., W. C. Tucker, …, J. C. Weisshaar. 2005. SNARE-driven, 25-millisecond vesicle fusion in vitro. *Biophys. J.* 89:2458–2472.

19. Kyoung, M., A. Srivastava, …, A. T. Brunger. 2011. In vitro system capable of differentiating fast Ca2+-triggered content mixing from lipid exchange for mechanistic studies of neurotransmitter release. *Proc. Natl. Acad. Sci. USA.* 108:E304–E313.

20. Talbot, W. A., L. X. Zheng, and B. R. Lentz. 1997. Acyl chain unsaturation and vesicle curvature alter outer leaflet packing and promote poly(ethylene glycol)-mediated membrane fusion. *Biochemistry.* 36:5827–5836.

21. Malinin, V. S., M. E. Haque, and B. R. Lentz. 2001. The rate of lipid transfer during fusion depends on the structure of fluorescent lipid probes: a new chain-labeled lipid transfer probe pair. *Biochemistry.* 40:8292–8299.

22. Stengel, G., R. Zahn, and F. Höök. 2007. DNA-induced programmable fusion of phospholipid vesicles. *J. Am. Chem. Soc.* 129:9584–9585.

23. Marsden, H. R., N. A. Elbers, …, A. Kros. 2009. A reduced SNARE model for membrane fusion. *Angew. Chem. Int. Ed.* 48:2330–2333.

24. Kashiwada, A., M. Tsuboi, and K. Matsuda. 2009. Target-selective vesicle fusion induced by molecular recognition on lipid bilayers. *Chem. Commun. (Camb.).* 6:695–697.

25. Chan, Y.-H. M., B. van Lengerich, and S. G. Boxer. 2008. Lipid-anchored DNA mediates vesicle fusion as observed by lipid and content mixing. *Biointerphases.* 3:FA17–FA21.

26. Chan, Y.-H. M., B. van Lengerich, and S. G. Boxer. 2009. Effects of linker sequences on vesicle fusion mediated by lipid-anchored DNA oligonucleotides. *Proc. Natl. Acad. Sci. USA.* 106:979–984.

27. Rawle, R. J., B. van Lengerich, …, S. G. Boxer. 2011. Vesicle fusion observed by content transfer across a tethered lipid bilayer. *Biophys. J.* 101:L37–L39.

28. Chen, X., D. Araç, …, J. Rizo. 2006. SNARE-mediated lipid mixing depends on the physical state of the vesicles. *Biophys. J.* 90:2062–2074.

29. Sutton, R. B., D. Fasshauer, …, A. T. Brunger. 1998. Crystal structure of a SNARE complex involved in synaptic exocytosis at 2.4 A resolution. *Nature.* 395:347–353.

30. Chung, M., R. D. Lowe, …, S. G. Boxer. 2009. DNA-tethered membranes formed by giant vesicle rupture. *J. Struct. Biol.* 168:190–199.

31. Takamori, S., M. Holt, …, R. Jahn. 2006. Molecular anatomy of a trafficking organelle. *Cell.* 127:831–846.

32. Chan, Y.-H. M., P. Lenz, and S. G. Boxer. 2007. Kinetics of DNA-mediated docking reactions between vesicles tethered to supported lipid bilayers. *Proc. Natl. Acad. Sci. USA.* 104:18913–18918.

33. Linderman, J. J., and D. A. Lauffenburger. 1986. Analysis of intracellular receptor/ligand sorting. Calculation of mean surface and bulk diffusion times within a sphere. *Biophys. J.* 50:295–305.

34. Schönherr, H., J. M. Johnson, …, S. G. Boxer. 2004. Vesicle adsorption and lipid bilayer formation on glass studied by atomic force microscopy. *Langmuir.* 20:11600–11606.

35. Hernandez, J. M., A. Stein, …, R. Jahn. 2012. Membrane fusion intermediates via directional and full assembly of the SNARE complex. *Science.* 336:1581–1584.

36. Simonsson, L., P. Jönsson, …, F. Höök. 2010. Site-specific DNA-controlled fusion of single lipid vesicles to supported lipid bilayers. *ChemPhysChem.* 11:1011–1017.

37. Aravanis, A. M., J. L. Pyle, and R. W. Tsien. 2003. Single synaptic vesicles fusing transiently and successively without loss of identity. *Nature.* 423:643–647.

38. Jackson, M. B., and E. R. Chapman. 2006. Fusion pores and fusion machines in Ca2+-triggered exocytosis. *Annu. Rev. Biophys. Biomol. Struct.* 35:135–160.

39. Malinin, V. S., and B. R. Lentz. 2004. Energetics of vesicle fusion intermediates: comparison of calculations with observed effects of osmotic and curvature stresses. *Biophys. J.* 86:2951–2964.

40. van Lengerich, B. 2012. DNA-mediated fusion of lipid vesicles. PhD dissertation. Stanford University, CA.

41. Floyd, D. L., J. R. Ragains, …, A. M. van Oijen. 2008. Single-particle kinetics of influenza virus membrane fusion. *Proc. Natl. Acad. Sci. USA.* 105:15382–15387.

42. Kasson, P. M., E. Lindahl, and V. S. Pande. 2010. Atomic-resolution simulations predict a transition state for vesicle fusion defined by contact of a few lipid tails. *PLOS Comput. Biol.* 6:e1000829.

43. Stevens, M. J., J. H. Hoh, and T. B. Woolf. 2003. Insights into the molecular mechanism of membrane fusion from simulation: evidence for the association of splayed tails. *Phys. Rev. Lett.* 91:188102-1–188102-4.

44. Grote, E., M. Baba, …, P. J. Novick. 2000. Geranylgeranylated SNAREs are dominant inhibitors of membrane fusion. *J. Cell Biol.* 151:453–466.

45. Stein, A., G. Weber, …, R. Jahn. 2009. Helical extension of the neuronal SNARE complex into the membrane. *Nature.* 460:525–528.

46. Ngatchou, A. N., K. Kisler, …, M. Lindau. 2010. Role of the synaptobrevin C terminus in fusion pore formation. *Proc. Natl. Acad. Sci. USA.* 107:18463–18468.

47. Lindau, M., B. A. Hall, …, M. S. P. Sansom. 2012. Coarse-grain simulations reveal movement of the synaptobrevin C-terminus in response to piconewton forces. *Biophys. J.* 103:959–969.

48. Chernomordik, L., A. Chanturiya, …, J. Zimmerberg. 1995. The hemifusion intermediate and its conversion to complete fusion: regulation by membrane composition. *Biophys. J.* 69:922–929.

49. Yang, L., and H. W. Huang. 2002. Observation of a membrane fusion intermediate structure. *Science.* 297:1877–1879.

50. Rizo, J., and C. Rosenmund. 2008. Synaptic vesicle fusion. *Nat. Struct. Mol. Biol.* 15:665–674.

51. Yoshina-Ishii, C., Y.-H. M. Chan, …, S. G. Boxer. 2006. Diffusive dynamics of vesicles tethered to a fluid supported bilayer by single-particle tracking. *Langmuir.* 22:5682–5689.

52. van Lengerich, B., R. J. Rawle, and S. G. Boxer. 2010. Covalent attachment of lipid vesicles to a fluid-supported bilayer allows observation of DNA-mediated vesicle interactions. *Langmuir.* 26:8666–8672.

53. Yoshina-Ishii, C., G. P. Miller, …, S. G. Boxer. 2005. General method for modification of liposomes for encoded assembly on supported bilayers. *J. Am. Chem. Soc.* 127:1356–1357.

54. Watkins, L. P., and H. Yang. 2005. Detection of intensity change points in time-resolved single-molecule measurements. *J. Phys. Chem. B.* 109:617–628.

Supporting Information

Individual Vesicle Fusion Events Mediated by Lipid-anchored DNA

Bettina van Lengerich*, Robert J. Rawle*, Poul Martin Bendix†, Steven G. Boxer

Department of Chemistry, Stanford University, CA 94305

†Current address: Niels Bohr Institute, Blegdamsvej 17, 2100 Copenhagen, Denmark

*Equal author contribution

Supporting Information Table of Contents

1. Supporting Materials and Methods

1.1 Preparation of dye-labeled DNA-lipids

DNA-lipids were prepared as in Ref. 1 by covalent attachment of a synthetic lipid-phosphoramidite as the final base to either the 3′ or 5′ end of an oligo on resin (sequences in Table S1), and subsequent purification on HPLC. For fluorescently labeled DNA-lipids, a C3-amino modifier was added during the DNA synthesis prior to the first base at the appropriate end (5′ or 3′, see Table 1). After coupling the lipid at the opposite end (3′ or 5′, respectively), the DNA was deprotected and cleaved from the resin, then the free amine was subsequently reacted with a dye-*N*-hydroxysuccinimide (NHS) ester to form the dye-labeled DNA-lipid, which was separated from excess dye on a PD-10 Sephadex desalting column (GE). This results in a dye-labeled DNA-lipid with a lipid at one end and a dye at the opposite end, so that the dye is attached to the DNA at the membrane-distal end. The labeling efficiency was calculated as the ratio of absorbance peak heights between the dye maximum and the DNA maximum (260nm), which was corrected for dye absorption at 260nm.   Labeling efficiencies for dye-DNA-lipids used in the current study are given in Table 1.

TABLE S1. DNA sequences and coupling orientations.

Name	Sequence (5' to 3')	% Labeled*
3'PolyA	AAA AAA AAA AAA AAA AAA AAA AAA - lipid	n/a
5'PolyA	lipid - AAA AAA AAA AAA AAA AAA AAA AAA	n/a
5'Poly A-Alexa488	lipid - AAA AAA AAA AAA AAA AAA AAA AAA - Alexa488	>100%
5'PolyT	lipid - TTT TTT TTT TTT TTT TTT TTT TTT	n/a
5'PolyT-Alexa546	lipid - TTT TTT TTT TTT TTT TTT TTT TTT - Alexa546	~85%
3'PolyT-Alexa546	Alexa546 - TTT TTT TTT TTT TTT TTT TTT TTT - lipid	>95%
Sequence 1	lipid - TAG TAT TCA ACA TTT CCG TGT CGA	n/a
Sequence 2	lipid - TCG ACA CGG AAA TGT TGA ATA CTA	n/a
Sequence 2-alkyne	alkyne- TCG ACA CGG AAA TGT TGA ATA CTA	n/a
3'Sequence 2	TCG ACA CGG AAA TGT TGA ATA CTA - lipid	n/a
Sequence 3	lipid - TCC TGT GTG AAA TTG TTA TCC GCA	n/a
Sequence 3-alkyne	lipid - TCC TGT GTG AAA TTG TTA TCC GCA - alkyne	n/a
Sequence 4	TGC GGA TAA CAA TTT CAC ACA GGA – lipid	n/a

* % Labeled calculated as the ratio of absorbance peak heights between the dye maximum and the DNA maximum (260nm), which was corrected for dye absorption at 260nm

1.2 Dynamic light scattering

Dynamic light scattering (DLS) measurements were performed on a Brookhaven 90 Plus machine, utilizing the Particle Sizing Software with the Zeta Pals option. Measurements were performed on freshly extruded vesicles (concentration ~0.3 mg lipids/mL in buffer that had been passed through a 0.03 μm polycarbonate filter to remove dust particles). Vesicles, prepared as in the lipid-mixing experiments with 2% TR-DHPE, were extruded at a pore size of 30 nm. The average hydrodynamic diameter was determined to be 48±12 nm (average ± standard deviation of the distribution, see Figure S1).
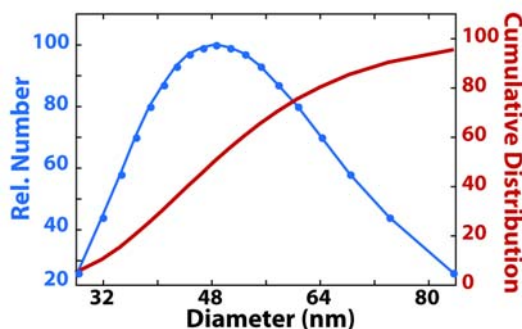

Figure S1. Distribution of vesicle sizes (hydrodynamic diameter) as measured by DLS for vesicles extruded at 30 nm. The relative number of vesicles (blue, scaled to 100) and cumulative distribution (red) are shown.

1.3 Image Acquisition and Processing

For the vesicle-to-tethered bilayer lipid mixing experiments, video streams of typically 1000-2000 frames were acquired with an acquisition time of 30 to 100 ms using 14-bit image settings for the lipid mixing experiment. The Texas Red labeled vesicles were excited using the Nikon Intensilight lamp and a 522-582 nm excitation filter, and the fluorescence was filtered through a 604-644 nm emission filter.

For the experiments using Alexa 546-labeled DNA-lipids, the dye was excited using a 532-550 nm excitation filter, and its fluorescence was filtered using a 572-642 nm emission filter. For the experiments measuring hybrid formation using Alexa 546-DNA-lipid and for the corresponding calibration curve, images were acquired with 144 ms acquisition time and using 16-bit image settings. For the single-step photobleaching

experiments using Alexa 546-DNA-lipid (see SI Section 10), images were acquired using 150 ms acquisition time, 2x2 binning, and 16-bit image settings.

1.4 Calculation of the Number of DNA Hybrids Formed ($N_{hybrids}$) in Dye-DNA Hybrid Formation Experiment (Fig. 3 and Fig. S11)

As discussed in the main text, there is a sharp increase in the local concentration of Alexa546-labeled DNA-lipid at the diffraction limited spot where the vesicle docks, due to hybridization of many fusion DNA pairs between the tethered patch and the docked vesicle. Fusion (or hemi-fusion) was detected by rapid disappearance of the bright spot due to the rapid dilution of the hybridized pairs into the membrane patch. Note that hemi-fusion and full fusion would both lead to complete dilution of the dye in the spot because the dye-labeled DNA in the hybrid is only on the outer leaflet of the vesicle (as drawn in Fig. 3A). Analysis of the hemi-fusion or fusion events was performed in a homemade Matlab program. Each trace was reviewed to ensure that only one docking event, and zero or one fusion event, occurred. An average background subtraction from a nearby (and unoccupied) region on the tethered membrane was applied to each vesicle so that the change in intensity upon docking could be measured accurately. The maximum integrated intensity of the vesicle before undergoing hemi/full fusion ($Intensity_{Vesicle}$) is proportional to the number of dye-labeled DNA-lipids gathered (i.e. number of DNA hybrids formed) by the docked vesicle (as shown in Fig 3B and 3C). The number of DNA hybrids formed $N_{hybrids}$ is calculated as

$$N_{hybrids} = \frac{Intensity_{Vesicle}}{Intensity_{Fluorophore}}$$

where the fluorescence intensity per fluorophore ($Intensity_{Fluorophore}$) is calculated from a calibration curve as described in SI Section 11 below.

2. Long Timescale Vesicle-to-Patch Fusion Experiment

In order to gain a qualitative understanding of the stability of the vesicles that were arrested at the docked or hemi-fused states, we performed a vesicle-to-tethered patch lipid mixing experiment in which the vesicles were observed over the course of many hours. An initial video micrograph of ~1 min was collected, during which vesicles were observed to dock and undergo fusion transitions (mostly hemi-fusion). Subsequent

to the video micrograph, time-lapse images of the docked and hemi-fused vesicles were acquired over the course of ~9 hours. Time-lapse images were taken at increasingly sparse time points to avoid photobleaching.
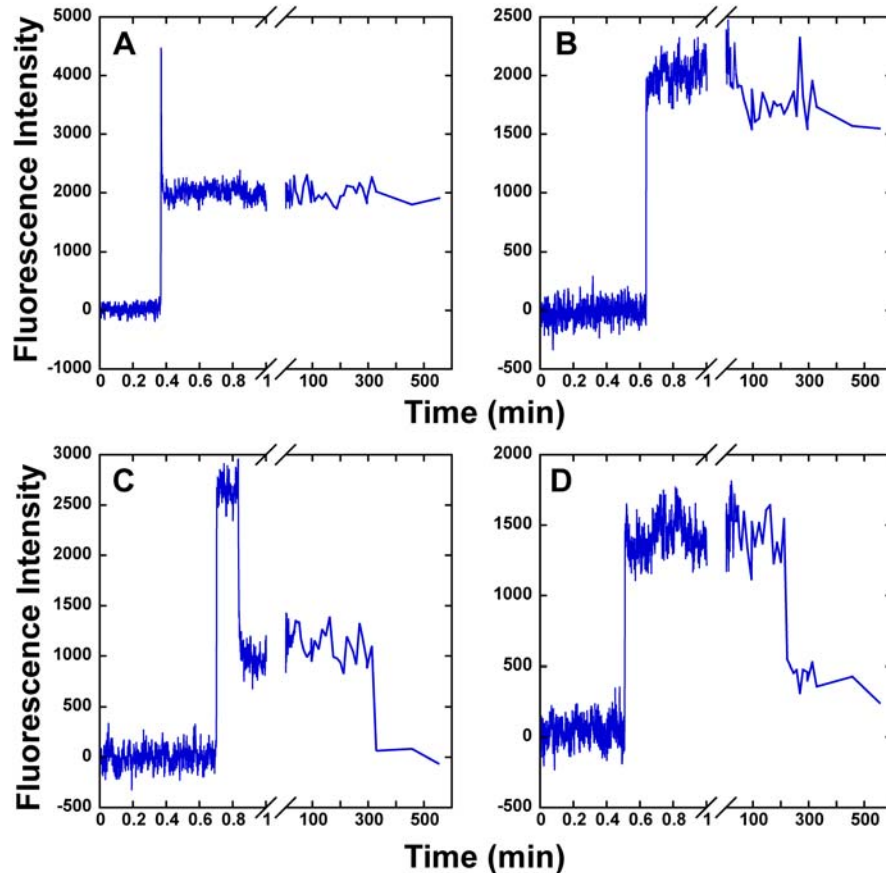

Figure S2. Example fluorescence intensity time traces showing various fusion behaviors that occurred over a very long time (hours) in a vesicle-to-tethered patch fusion experiment, 195 DNA/vesicle on average. (A) Arrested hemi-fusion—a vesicle docks and almost immediately hemi-fuses at ~0.4 min, then remains stably hemi-fused for the duration of the experiment. (B) Arrested docking—a vesicle docks at ~0.6 min and undergoes no further change. (C) Fast hemi-fusion, full fusion much later—a vesicle docks at ~0.7 min, undergoes hemi-fusion at ~0.8 min, and then transitions to full fusion at ~300 min. (D) Hemi-fusion after a long waiting period—a vesicle docks at ~0.5 min, hemi-fuses at ~200 min, and then remains stably hemi-fused for the duration of the experiment. Note the change in timescale and density of data points before and after the break in the x-axis.

We observed that both the docked and hemi-fused vesicles could be quite stable. Figure S2A and S2B show example traces of vesicles which were stably hemi-fused or stably docked over ~9 hours. Some stably docked or hemi-fused vesicles did eventually undergo full or hemi-fusion after many hours. Figure S2C shows an example trace of a

hemi-fused vesicle which underwent full fusion after ~5 hours and Figure S2D shows the trace of a docked vesicle which eventually hemi-fused after ~3 hours.
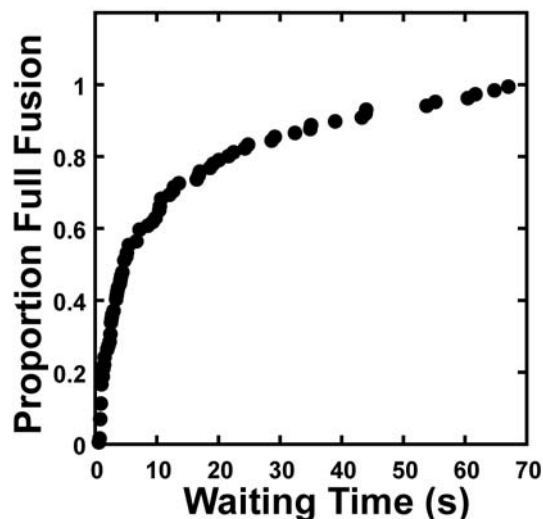
3. Full Fusion Kinetics

Figure S3. CDF of the docking to full fusion wait times for events identified as full-fusion-only in vesicle-to-tethered membrane lipid-mixing experiments. Because full-fusion-only events were so rare, we compiled events from several different data sets in order to generate the CDF. Mean wait time = 15 sec, N = 68.

4. Distribution of DNA-lipids in Vesicles

The actual distributions of DNA-lipids in vesicles (Figure S4) were determined by incorporating a dye-DNA-lipid (3'PolyT-Alexa546) at varying DNA/vesicle number densities into vesicles which contained a very small amount of Oregon Green-DHPE lipid dye (<0.1 mole percent, equivalent to ~25 dyes/vesicle). Vesicles were adhered to a glass slide at low density such that hundreds of individual vesicles could be easily distinguished in a widefield epifluorescence image. The Oregon Green (OG) fluorescence and Alexa546 fluorescence for each set of vesicles was captured. The OG intensity was used to identify vesicles and the Alexa546 intensity of each vesicle was used to calculate its number of DNA-lipids. Both intensities were quantified by a homemade MATLAB program which performed a 2D Gaussian fit for each vesicle in order to calculate the local background signal, which was subtracted from the integrated fluorescence intensity. The small amount of OG was not enough to produce any significant bleedthrough into the Alexa546 image. To translate the Alexa546

intensity/vesicle into number of Alexa546 dyes/vesicle (and consequently number of DNA-lipids/vesicle), stepwise photobleaching of Alexa546 was performed on many vesicles containing a low number of DNA/vesicle and the average step size (i.e. fluorescence intensity/Alexa546 dye) was calculated (c.f. Figure S10).
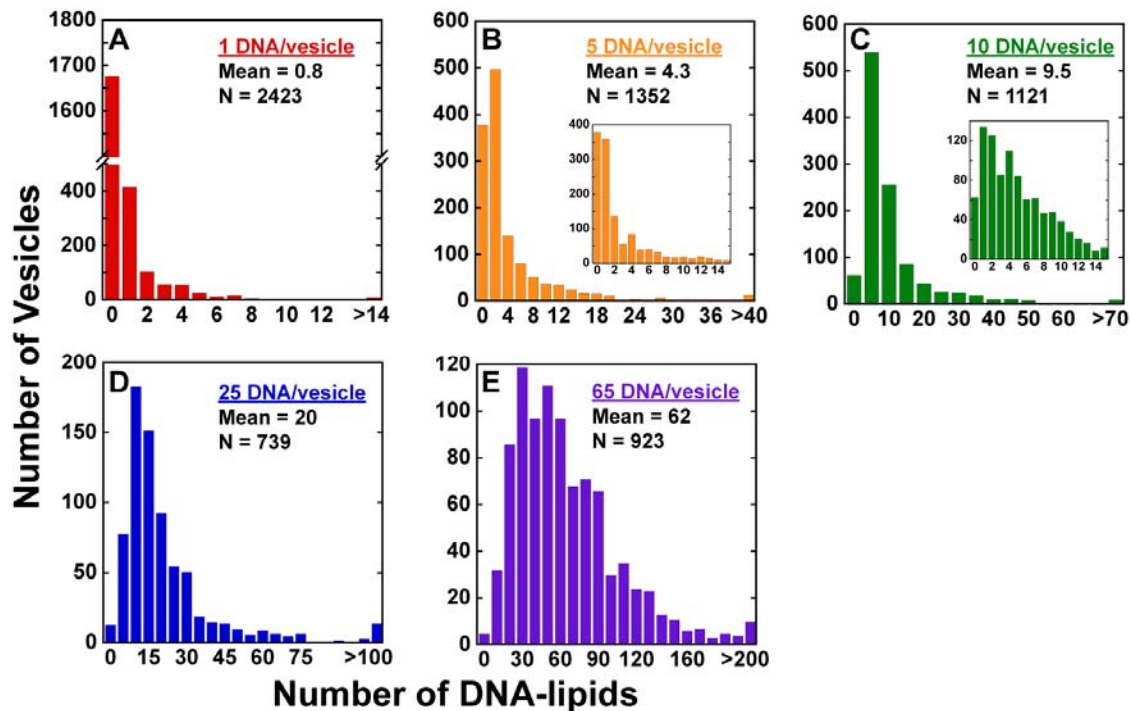

Figure S4. The observed distributions of DNA-lipids in vesicles to which on average were added (A) 1 DNA/vesicle, (B) 5 DNA/vesicle, (C) 10 DNA/vesicle, (D) 25 DNA/vesicle, or (E) 65 DNA/vesicle. The observed mean of each distribution is reported as well as the total number *N* of vesicles observed.

The observed mean DNA/vesicle number densities were very close to the expected average number densities which had been added to the vesicles (calculated using the average size of the vesicle, 48±12 nm in diameter, as determined by DLS—see Fig. S1), indicating that the DNA-lipids were inserting quantitatively[1]. However, the distributions each had very long tails, much longer than what would be expected from Poissonian statistics. This suggests that entire DNA-lipid micelles might occasionally

---

[1] At higher DNA/vesicle number densities (> 0.5 mole% DNA-lipid, which corresponds to ~125 DNA/vesicle for a 50 nm vesicle), we have observed that the DNA-lipids no longer insert quantitatively. This can be seen quite easily in the characterization method described above as many Alexa546 spots (presumably micelles of 3'PolyT-Alexa546) which are not co-localized with any Oregon Green signal (i.e. not co-localized with any vesicle). At the DNA/vesicle number densities used in this report, these micelles are seen only infrequently, consistent with the conclusion that the DNA-lipids have inserted quantitatively.

fuse with vesicles during the insertion process, generating the long tails in the distributions.

5. Modeling of Docking to Hemi-fusion Wait Times by Maximum Likelihood Estimation

The cumulative distribution functions (CDF) of the docking to hemi-fusion waiting times exhibited exponential behavior in all of our experiments, suggesting that the docking to hemi-fusion transition is a Poissonian process. Within the time resolution of those experiments, we never observed a lag at the beginning of the CDFs which would suggest that there might be multiple rate-limiting steps between docking and hemi-fusion (see Discussion in main text).

Using maximum likelihood estimation (MLE), we found that most of our data was modeled well by a single exponential distribution of the form $CDF(t) = 1 - e^{-t/\tau_{wait}}$, where τ_{wait} is the parameter varied in the MLE and represents the mean wait time of the fit. Example fits to this distribution are shown in Figure S5 (black line) and Figure 2A in the main text (black line).
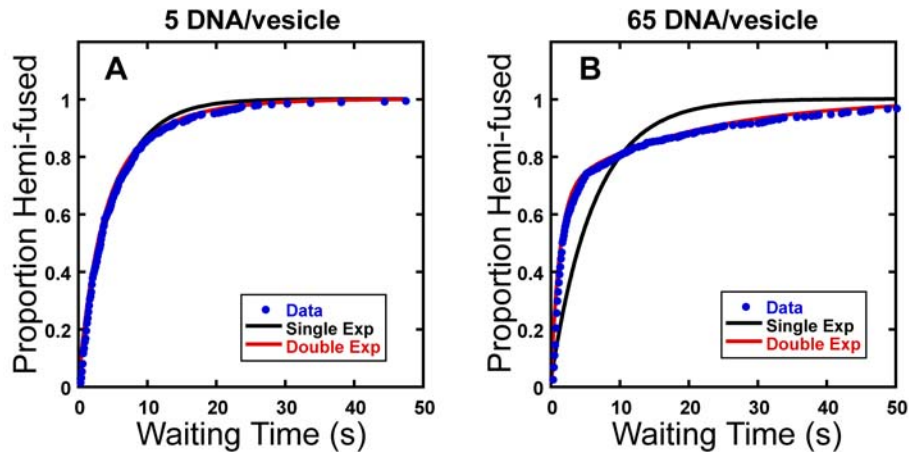

Figure S5. Example fits of a single or double exponential distribution to the docking to hemi-fusion waiting time cumulative distributions for (A) 5 DNA/vesicle and (B) 65 DNA/vesicle number densities (poly A/ poly T DNA sequence). This is the same data as shown in Figure 2B of the main text.

Interestingly, when we examined the dependence of the docking to hemi-fusion rate on DNA/vesicle number density for the poly A/ poly T sequence (Figure 2B in main text), we found that the CDFs for 25 and 65 DNA/vesicle were not as well modeled by a

single exponential distribution (see Figure S5(B)). These CDFs were, however, well modeled by a double exponential distribution of the form $CDF(t) = 1 - A_1 e^{-t/\tau_1} + A_2 e^{-t/\tau_2}$. This distribution would suggest that a slow and a fast fusing population may exist. In that case, A_1 and A_2 would represent the proportion of data that fell into either population and τ_1 and τ_2 would be their respective mean waiting times. Indeed the CDFs shown in Figure 2B of the main text look as though a slow population may contribute more strongly at the higher number densities (25 and 65 DNA/vesicle).

An explanation consistent with this observation would be that vesicles with a higher DNA/vesicle number density may be more likely to have a DNA-lipid become trapped between the vesicle and the target membrane during docking, arresting fusion until the trapped DNA-lipid can escape. In support of that explanation is the observation that vesicles with 25 and 65 DNA/vesicle were mostly immobile upon docking (presumably mobile vesicles are less likely to have a DNA-lipid become trapped between the two membranes). Also, we observed an apparent increase in docking-only events at higher DNA/vesicle number densities, which would be expected if this explanation were correct (data not shown). On the other hand, the CDFs for the high DNA/vesicle number densities for the fully overlapping Sequence 1 & 2 did not show a similar trend away from a single exponential distribution (see Figure S6), nor did the data in Figure 2A (75 DNA/vesicle, poly A/poly T DNA sequence).

Ultimately, we decided not to pursue experiments that might tease out the source of this deviation away from a single exponential distribution because the overall change in kinetics was modest at best across the different DNA/vesicle number densities. It seemed likely that experiments designed to extract the source of the slightly different kinetic behaviors could easily be confounded by experimental noise. Our central observations are that changing the DNA/vesicle number density across a very wide range (1 to 65 DNA/vesicle) did not alter the kinetic behavior significantly and that no lag time was observed in the CDFs for any of our data sets.

6. Vesicle-to-Patch Fusion Experiments Using Fully Overlapping DNA Sequences
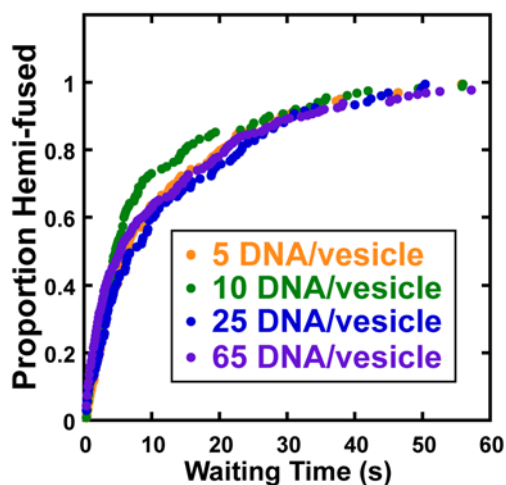

Figure S6. Cumulative distributions of the docking to hemi-fusion wait times for vesicle-to-tethered patch lipid mixing experiments using the fully overlapping Sequence 1 & 3'Sequence 2 (see Table S1) to mediate fusion. The DNA/vesicle number density was varied from 5 to 65 DNA/vesicle and the DNA density in the tethered patch was held constant at 0.5 mole %. Because of the decreased docking rate at low number densities, it was not practical to collect data at 1 DNA/vesicle for this DNA sequence. Statistical information for each DNA/vesicle number density is given in Table 1 in the main text.
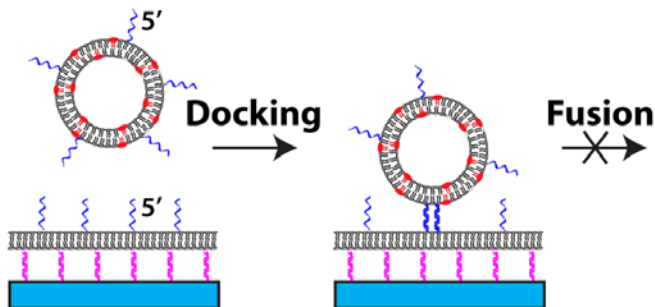
7. Importance of DNA Binding Orientation

Figure S7. Schematic of vesicle-to-tethered membrane fusion experiment where the DNA-lipids in both vesicle and target membrane are coupled to their respective lipid anchors on the 5' end of the DNA (tethering orientation). Hybridization in this case will locally hold the apposing membranes apart by the length of the DNA duplex (8 nm in our experiments). We observed that this tethering orientation prevented any fusion transitions (hemi-fusion or full fusion) following the docking event.

The importance of DNA binding orientation was determined by performing a vesicle-to-tethered bilayer lipid mixing experiment, where the DNA-lipids on both membrane surfaces were anchored to the membrane at their 5' end (5' PolyA and 5' PolyT sequences, see Table S1), rather than on the 3' end on one surface and the 5' end on the other (zippering orientation), as is the case for all the other fusion experiments described

in this report. Upon hybridization, this tethering orientation should locally keep the vesicle and target membranes apart by the length of the ~8 nm 24mer duplex (see schematic in Figure S7), rather than bringing them close together, as is the case for the zippering orientation. We observed that docking, but not fusion, occurred when the tethering orientation was used to dock the incoming vesicles to the patch (data not shown). Similar to the experiments performed with the zippering orientation, the docked vesicles were mobile at a low DNA-lipid number density in the vesicle, while at a high number density they were immobile, suggesting that more hybrids had formed (see mobility discussion in SI Section 8). In both cases, no fusion behavior was observed to occur. Overall, this indicates that the correct binding orientation is essential in order to allow fusion to proceed.

8. Mobility of DNA-tethered Vesicles

In previous reports (2, 3) we have extensively examined and characterized the mobility of vesicles tethered by DNA-lipid conjugates to glass supported bilayers (SLB), where the DNA tethers were hybridized in the tethering orientation (i.e. conjugate DNA-lipids were both anchored at the 5' end). In one of those reports (2), we found that the average diffusion coefficient of tethered vesicles was not significantly different for vesicles with a high number of DNA/vesicle (25 DNA per 100 nm vesicle) as compared with a low number of DNA/vesicle (0.1 DNA per 100 nm vesicle). This suggested that only one DNA-lipid was anchoring the vesicle to the SLB, even if the vesicle contained more than one DNA-lipid. This report is in apparent contradiction with the observation in the present report that the mobility of vesicles docked to DNA-tethered membrane patches was reduced and ultimately abolished as the number of DNA/vesicle was increased (see SI Section 7 and Movie S3).

Since the differing mobility of vesicles is not the focus of the current report, we have not quantified the average diffusion coefficients of docked vesicles herein, however several qualitative observations about differences between the current and previous methods may clarify the apparent discrepancy. First, the differences between DNA-tethered membrane patches and SLBs are not sufficient to explain the difference in mobility. In follow-up experiments (data not shown), we have observed the change in

vesicle mobility as a function of DNA/vesicle number density for both tethered patches and SLBs. Second, DNA binding orientation is not sufficient to explain the difference— we observed similar behavior for vesicles docked in both the tethering and the zippering orientations, although the effect was more pronounced for the zippering orientation, as might be expected. Third, there are subtle differences in the chemistry linking DNA to the lipid and in the lipid composition compared to the previous reports. The DNA-lipid linkage used in ref. 2 was based on *in situ* thiol/maleimide coupling chemistry (see ref 4) while that in the current report is based on phophoramidite chemistry (see ref 1); this more recent approach gives much greater control over the number of DNA-lipids/vesicle. The lipid composition of the vesicles was also different—EggPC in ref. 2 and 2:1:1 DOPC:DOPE:Chol in the current report. However, neither of these differences is expected to account for the observed difference in mobility.

The most likely candidate to explain the apparent discrepancy is that the DNA-lipids used in this report are primarily the polyA/polyT pairs whereas those in the previous reports are fully overlapping sequences. In both tethering and zippering orientations, we have consistently observed that the fully overlapping sequences are more mobile at a given number density of DNA-lipids as compared to the polyA/polyT pairs. This is likely due to the ability of the repeating polyA/polyT sequences to hybridize with only partial overlap between partner strands, something unlikely to occur for a fully overlapping sequence. In the tethering orientation (the relevant comparison between this and the previous reports), this ability may allow enough hybrids to form between vesicle and the underlying membrane to significantly reduce or abolish mobility.

While the previous report (2) demonstrated that the size of the tethered vesicle did not affect its mobility, we have not as yet examined the combined effect of DNA/vesicle number density and vesicle size, and that may also explain somewhat the differing results (in the previous report, where the dependency on DNA/vesicle number density was not the principal focus, we only compared 0.1 DNA/vesicle with 25 DNA/vesicle for nominally 100 nm vesicles, while in the current report we have dealt exclusively with 50 nm vesicles across a wide range of DNA/vesicle number densities).

9. Transfer of DNA-lipids from Vesicle to Tethered Membrane During Hemi- or Full Fusion
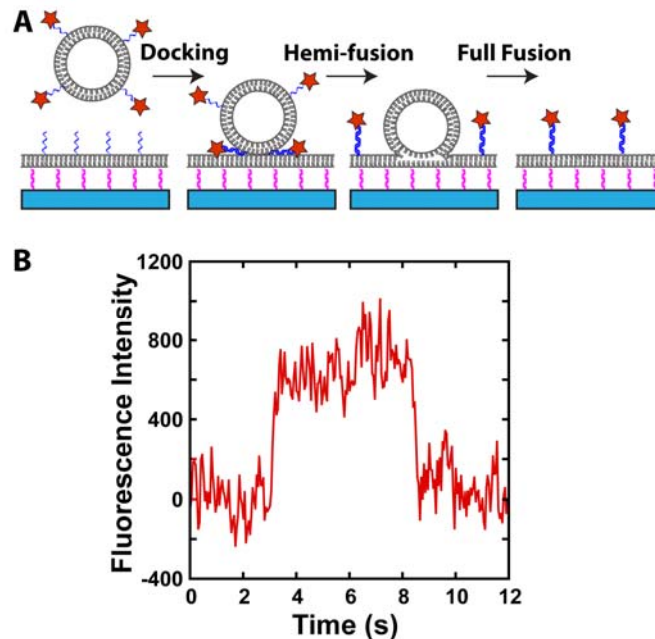

Figure S8. (A) Schematic of a vesicle-to-tethered membrane fusion experiment in which fusion is monitored as the transfer of dye-DNA-lipids (red stars) from vesicle to unlabeled tethered membrane. The dye-DNA-lipid is contained only in the outer leaflet of the vesicle. (B) Example fluorescence time trace of a vesicle with dye-labeled DNA-lipids (3'Sequence 2-Alexa546, 125 DNA/vesicle) docking (at t=3s) and fusing (at t=8s) to a target tethered membrane patch (Sequence 1, 0.5 mole %). When the vesicle fuses to the target membrane (likely hemi-fusion), the dye is completely transferred to the membrane patch indicating that all DNA-lipids are transferred to the target membrane during hemi-fusion (or full fusion). This event (as well as others) is shown in Movie S4. Time t=0 is arbitrary.

To confirm that the DNA-lipids on the vesicle are fully transferred to the tethered bilayer upon hemi-/full fusion, we performed two experiments. In the first, shown in Figure S8, dye-labeled DNA-lipids are incorporated into the vesicle and their fluorescence is used to monitor docking and hemi/full fusion. For essentially all fusion events in this experiment, we observed that, after a short waiting time following docking, the fluorescence signal from the dye-DNA-lipid was transferred completely into the target membrane patch. Partial transfer events were rarely observed. Consistent with the expectation that the DNA-lipid is displayed only on the outside of the vesicle, this result indicates that upon hemi-/full fusion, all DNA-lipids (hybridized or not) from the SUV rapidly diffuse into the tethered target membrane and become diluted.
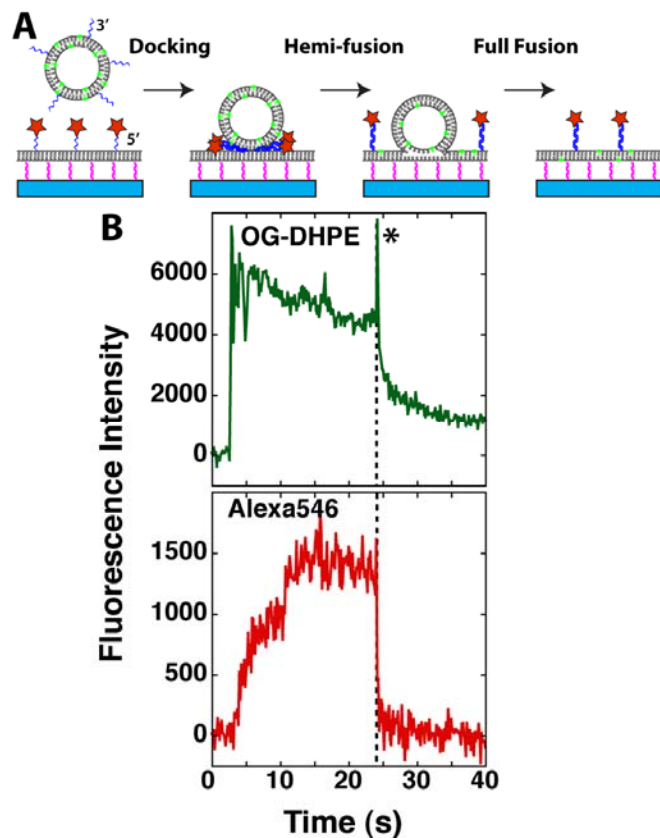
Figure S9. (A) Schematic of a fusion experiment in which DNA hybridization and lipid mixing are monitored simultaneously. The DNA in the tethered membrane (0.01%, Alexa546-5'PolyT) is labeled with Alexa-546 at its membrane distal end (red stars). The incoming vesicle displays 3'PolyA (65 DNA/vesicle) and is labeled with Oregon Green-DHPE lipids (5 mole%). (B) Example fluorescence time trace of the OG-DHPE signal (green trace, background subtracted) and Alexa546 signal (red trace, background subtracted and corrected for cross-talk) during a hemi-fusion event. The vesicle docks at t=4s and hemi-fuses at t=24s as shown in the lipid-mixing (green) trace. When the vesicle hemi-fuses, the Alexa546 signal abruptly disappears, indicating that all hybridized DNA pairs are able to freely diffuse away from the vesicle into the much larger membrane patch area. Time t=0 is arbitrary. * indicates dequenching of OG upon hemi-fusion.

In the second experiment, shown schematically in Figure S9A, DNA hybrid formation and lipid-mixing were monitored simultaneously. The two-color fluorescence time trace in Figure S9B shows an example hemi-fusion event. Upon docking at t=4 s (indicated by abrupt appearance of the vesicle in the OG-DHPE channel), the vesicle slowly forms DNA hybrids with target tethered membrane (Alexa546 trace) until a maximum number is reached around t=12 s. Upon hemi-fusion at t=24 s (detected as incomplete loss of OG-DHPE signal) the Alexa546 signal simultaneously disappears. Similar behavior was observed for all hemi-fusion events in this experiment, indicating that all DNA hybrids formed between vesicle and tethered membrane are able to freely

diffuse away from the hemi-fused vesicle immediately upon membrane merger. Note that the spike in the OG-DHPE signal upon hemi-fusion (indicated with *) is due to fluorescent dequenching of the OG dye. OG was included at a self-quenched concentration (5 mole%) in the vesicle because of its propensity to photobleach over the length of an average experiment.

10. Calibration of the Number of DNA Hybrids Formed at a Docked Vesicle

To quantitatively relate spot intensity to the number of DNA duplexes (SI Section 1.4), we constructed a calibration curve by depositing vesicles containing a very low number density of dye-labeled DNA-lipid on a glass coverslip and determining the intensity per fluorophore by single step photobleaching (Fig. S10). The intensities of vesicles with higher number densities of dye-labeled DNA-lipids were also measured, demonstrating that the dependence of the average intensity per vesicle on number density of DNA-lipid was linear up to 65 DNA/vesicle (data not shown).
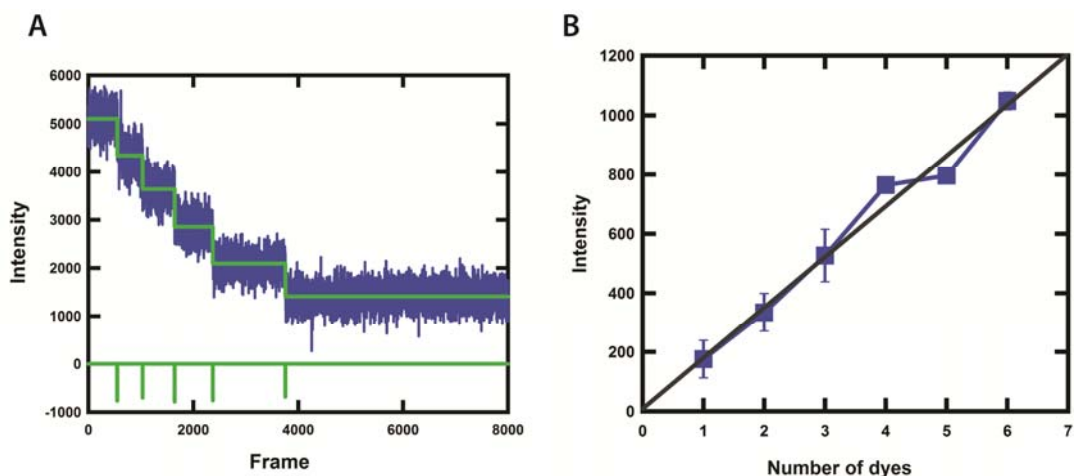

Figure S10. (A) Single step photobleaching of a vesicle prepared with 0.01 mole % Alexa 546-DNA-lipid (blue trace). The green trace is a fit to a change point function based on Ref. 5, and its gradient. (B) Fluorescence intensity of vesicles as a function of the number of fluorophores. The slope of the line determines the intensity per fluorophore. The step sizes were similar for each photobleaching step (data not shown). Note that different acquisition settings were used to acquire data in A and B, hence the intensity per step is different.

One potential issue with this type of calibration curve is that the fluorescent dye molecule may be very sensitive to the environmental differences between the conditions under which the hybrid formation data was collected (vesicles docked to a tethered

membrane patch) and the conditions under which the data for the calibration curve was collected (vesicles adsorbed to a glass surface). For example, the hybridized DNA may assume a more horizontal orientation (i.e. more parallel to the lipid bilayer) at a docked vesicle and this orientation change may alter its observed fluorescence intensity due to polarization effects. Ideally, the calibration curve would be collected under conditions nearly identical to those of the actual experiment (i.e. vesicles docked to a tethered membrane patch). Unfortunately, auto-fluorescent background of the tethered membrane patches makes single-step photobleaching experiments technically challenging for that system. Therefore, it became necessary to verify that the environmental differences between the calibration curve and the hybrid formation experiment did not significantly affect the fluorescence of the dye-DNA-lipid.

In order to examine the effect of those environmental differences, a glass-supported bilayer was used as the target membrane in order to approximate the environment of a tethered membrane patch. Vesicles containing dye-DNA-lipid (at a low number density of dye-DNA/vesicle to guarantee that all DNA on the vesicle would be hybridized) were allowed to dock to the unlabeled glass-supported lipid bilayer displaying the complementary DNA. The bilayer was composed entirely of EggPC lipids—a composition that does not allow fusion to proceed (i.e. all vesicles are docking-only)—which permitted stable imaging of the docked vesicles. The intensities of these docked vesicles were then compared side-by-side to vesicles from the same stock that were adsorbed to a glass surface at high dilution. The ratio of the slopes of these two calibration curves was approximately 1.1 (data not shown), indicating that the environmental differences did not significantly affect the dye fluorescence.

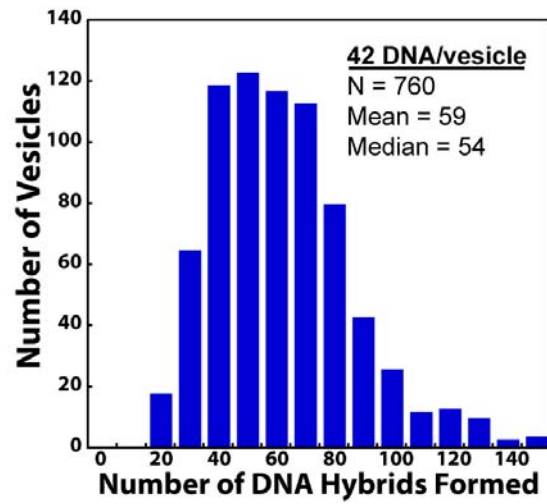## 11. Number of DNA Hybrids Formed for Vesicles with 42 DNA/vesicle

Figure S11. Distribution of the number of DNA hybrids formed between vesicles (42 DNA/vesicle added on average) and a tethered patch before undergoing hemi- or full fusion. Number of DNA hybrids formed is calculated from the fluorescence intensity of the docked vesicle before fusion, using a suitable calibration curve (see SI Section 10 above).

12. Supporting Movie Information

Movie S1. Example Hemi-then-full fusion event in vesicle-to-tethered patch lipid mixing experiment.

Movie S2. Example Full Fusion only event in vesicle-to-tethered patch lipid mixing experiment.

Movie S3. A comparison of the mobility of vesicles with 1, 10, and 65 DNA/vesicle in separate vesicle-to-tethered patch lipid mixing experiments.   Hemi-fusion events are captured in each movie.

Movie S4. Transfer of Alexa546-DNA-lipid from vesicle to patch.   Trace is shown in Fig. S8.

13. Supporting References

1. Chan, Y-H.M., B. van Lengerich, S.G. Boxer. 2008. Lipid-anchored DNA mediates vesicle fusion as observed by lipid and content mixing. Biointerphases 3:FA17-FA21.

2. Yoshina-Ishii, C., Y-H.M. Chan, J.M. Johnson, L.A. Kung, P. Lenz, S.G. Boxer. 2006. Diffusive dynamics of vesicles tethered to a fluid supported bilayer by single-particle tracking. Langmuir. 22:5682-5689.

3. van Lengerich, B., R.J. Rawle, S.G. Boxer. 2010. Covalent attachment of lipid vesicles to a fluid-supported bilayer allows observation of DNA-mediated vesicle interactions. Langmuir. 26:8666-8672.

4. Yoshina-Ishii, C., G.P. Miller, M.L. Kraft, E.T. Kool, S.G. Boxer. 2005. General Method for Modification of Liposomes for Encoded Assembly on Supported Bilayers. J. Am. Chem. Soc. 127:1356-1357.

5. Watkins, L.P., H. Yang. 2005. Detection of intensity change points in time-resolved single-molecule measurements. J. Phys. Chem. B. 109:617-628.